Developmental Timing of High-Fat Diet Exposure Impacts Glucose Homeostasis in Mice in a Sex-Specific Manner

Maria M. Glavas,[1] Ann Y. Lee,[1] Ian Miao,[1] Fan Yang,[1] Majid Mojibian,[1] Shannon M. O'Dwyer,[1] and Timothy J. Kieffer[1,2,3]

We previously demonstrated that male, but not female, Swiss Webster mice are susceptible to diabetes, with incidence increased by early overnutrition and high-fat diet (HFD). In this study, we investigated how HFD in Swiss Webster males and females during preweaning, peripubertal, and postpubertal periods alters glucose homeostasis and diabetes susceptibility. In males, HFD throughout life resulted in the highest diabetes incidence. Notably, switching to chow postpuberty was protective against diabetes relative to switching to chow at weaning, despite the longer period of HFD exposure. Similarly, HFD throughout life in males resulted in less liver steatosis relative to mice with shorter duration of postpubertal HFD. Thus, HFD timing relative to weaning and puberty, not simply exposure length, contributes to metabolic outcomes. Females were protected from hyperglycemia regardless of length or timing of HFD. However, postpubertal HFD resulted in a high degree of hepatic steatosis and adipose fibrosis, but glucose regulation and insulin sensitivity remained unchanged. Interestingly, peri-insulitis was observed in the majority of females but was not correlated with impaired glucose regulation. Our findings reveal critical periods of HFD-induced glucose dysregulation with striking sex differences in Swiss Webster mice, highlighting the importance of careful consideration of HFD timing relative to critical developmental periods.

Consumption of an obesogenic diet is associated with metabolic dysfunction, including obesity and impairments in glucose homeostasis that can lead to diabetes (1). Intuitively, longer exposure to an obesogenic diet is expected to be more detrimental. However, the developmental time period of diet exposure is an additional key factor to consider since tissues and organ systems may be more susceptible to an adverse nutritional environment during periods of rapid growth. Long-term detrimental effects of adverse prenatal and perinatal environments, the so-called Developmental Origins of Health and Disease hypothesis, have long been recognized particularly in relation to undernutrition, which increases incidence of obesity and type 2 diabetes in offspring (2,3). Similarly, prenatal exposure to maternal obesity, high-fat diet (HFD), and diabetes increase offspring risk of developing obesity and diabetes (4,5). With human studies, it is difficult to isolate the role of early postnatal nutrition from potential confounding effects of prenatal environment and genetics. However, studies in rodents have shown that exposure to overnutrition and HFD that is limited to the lactation/preweaning period (first 3 weeks of life) can lead to lifelong impairments in glucose homeostasis and increased adiposity (6–13). Although most studies have been conducted in the inbred C57BL/6 strain and in males only, Masuyama and Hiramatsu (8) found that both male and female adults of the outbred ICR mouse strain had impaired glucose and insulin tolerance after HFD exposure during the preweaning period, while Hafner et al. (14) found that only male C57BL/6 but not female mice had impaired glucose and insulin tolerance,

METABOLISM

suggesting strain differences in sex effects. Notably, 8-week-old male offspring from dams exposed to HFD only during lactation exhibited reduced hypothalamic densities of α–melanocyte-stimulating hormone and agouti-related peptide fibers, indicating long-term effects on hypothalamic neurocircuitry critical for energy homeostasis, as well as decreased parasympathetic outputs to islets (11); however, females were not examined. In line with the importance of offspring nutrient exposure during preweaning, we previously showed that overnutrition during this period, induced by reducing the litter size, increased susceptibility to diabetes in male, but not female, Swiss Webster mice and that this was exacerbated by HFD exposure (15,16). Together, these studies indicate that the preweaning period is a critical time for programming body composition and glucose homeostasis.

Numerous studies have examined long-term effects of HFD exposure in the prenatal and early postnatal periods; however, there is a paucity of studies specifically examining the effects of dietary fat content in diets initiated at weaning. In rodents, weaning onto standard chow typically results in a significant decrease in dietary fat intake, from ~55% of calories from fat in maternal milk to 10–20% with chow. The World Health Organization recommends dietary fat intake constitute <30% of daily calories (17), while an obesogenic western diet in humans may constitute 35–60% fat. Thus, infants transitioning to solid food may experience varying degrees of shift in dietary macronutrient composition, including fat content, depending on the diet. However, whether a dramatic shift in diet composition is beneficial or detrimental to developing metabolic systems is unclear.

The final major developmental period is puberty. Given the extensive cross talk among endocrine tissues, the dramatic changes in sex hormones during puberty subsequently give rise to alterations throughout the endocrine system. Of relevance to glucose regulation, transient insulin resistance is observed during puberty in humans with lower insulin sensitivity in girls than boys, although the underlying mechanisms are unclear (18,19). Obesity during puberty further exacerbates insulin resistance, and overweight during puberty is associated with a higher incidence of type 2 diabetes in adulthood even when heavier body weight resolves (19,20). However, there is a scarcity of data on the role that dietary fat may play on glucose regulation during puberty. With diet-induced mouse models of obesity and glucose intolerance, HFD exposure is often initiated at 6–10 weeks of age since some studies have shown that initiating HFD immediately after weaning or during the peripubertal period may attenuate detrimental metabolic effects (21,22). These observations suggest that puberty may be a critical developmental period for HFD-mediated metabolic impairments.

Given the many unanswered questions regarding dietary fat exposure in relation to weaning and puberty, we took an unbiased approach to explore the impact of HFD during three broad postnatal periods designated as the preweaning period from postnatal day (P) 2 to 21, the peripubertal period from P21 to 35, and the postpubertal period from P35 onwards, with HFD exposure limited to either zero, one, two, or all three of these periods, resulting in eight different groups. We chose to conduct these studies in the outbred Swiss Webster mouse strain, as we have previously observed that Swiss Webster males are susceptible to HFD and early overnutrition-induced β-cell dysfunction and diabetes (15,16). Moreover, the superior nurturing traits of Swiss Webster dams ensures consistent nutrition for suckling pups and thus minimizes variation due to maternal behavior. Examination of resulting body weight gain, glucose regulation, and diabetes susceptibility in offspring revealed critical periods of HFD-induced glucose dysregulation, diabetes susceptibility, and liver steatosis, as well as striking sex differences in Swiss Webster mice.

RESEARCH DESIGN AND METHODS

Animals and Diets

Diets were modified (either chow or HFD) during three broad periods in offspring: preweaning, P2–21; peripubertal, P21–35; and postpubertal, P35 onward as illustrated in Supplementary Fig. 1. First, pregnant Swiss Webster females (Taconic Biosciences, Rensselaer, NY) were maintained on chow diet (13 kcal% fat; NIH-31M; Ziegler Bros., Gardners, PA). Two days postdelivery (P2 for pups), litter size was adjusted to 10 pups to ensure consistent nutrition among litters, and half of the dams were switched to HFD (45 kcal% fat; #D12451; Research Diets, Inc., New Brunswick, NJ). Offspring were weaned at P21 and either remained on the same diet as their mother or had their diet switched (chow to HFD or vice versa). At P35, offspring either remained on the same diet or underwent a diet switch (from chow to HFD or vice versa). This resulted in eight diet groups in which group names indicate the period of HFD exposure (otherwise chow diet was consumed): CHOW, $HFD^{P21–35}$, $HFD^{P2–21}$, $HFD^{P2–35}$, HFD^{P35+}, HFD^{P21+}, $HFD^{P2–21,P35+}$, and HFD^{P2+}. Although we did not systematically evaluate puberty onset (e.g., by day of vaginal opening in females and balanopreputial separation in males), several studies have shown earlier onset in response to HFD and wide differences among strains (23–26). Thus, we chose a larger window of P21–35 for our peripubertal period to cover a wide range of onset. Mice also show a second growth spurt around this time (~P20–33), after an earlier perinatal growth spurt that ends at ~P16 (27); thus, we hypothesized that during this time period mice may be more sensitive to dietary changes. Two independent cohorts were generated. In cohort 1, only male mice were monitored to 6 months. In cohort 2, both males and females were studied, with a subset euthanized at P35 (with no diet change at P35). Remaining males were euthanized at P72 to obtain adult tissues without the potential

confounding effects of high diabetes incidence that would be more likely at a later age. Females were monitored up to P325. Although the initial plan was to monitor female mice to 6 months, as we did for males, we observed some cases of hyperglycemia in females and therefore followed females to 1 year in case diabetes in females occurred at a later age. Mice were housed in Optimice cages (Animal Care Systems, Centennial, CO) in a barrier facility (Centre for Disease Modeling, University of British Columbia Life Sciences Institute) with a 12-h light/12-h dark cycle and controlled temperature and humidity. All mice had ad libitum access to food and water as well as shelter huts, cotton nestlets, and crinkle paper. All animal procedures were approved by the University of British Columbia Animal Care Committee and carried out in accordance with the Canadian Council of Animal Care guidelines.

Glucose Monitoring
Beginning at P30, 4-h fasted blood glucose measures were taken weekly from the saphenous vein using a OneTouch Ultra 2 glucometer (LifeScan, Burnaby, British Columbia, Canada). Note that the coefficient of variation of glucose measures with this glucometer is estimated at 9.3% (28). Day of diabetes onset was defined as the first 4-h fasted glucose value ≥20 mmol/L and confirmed by a second fasting glucose value ≥20 mmol/L the following week. For oral glucose tolerance tests, mice were fasted for 6 h and glucose (2 g/kg) administered by oral gavage with glucose measured at 0, 10, 20, 30, 60, 90, and 120 min. For insulin tolerance tests, mice were fasted for 4 h and 0.75 units/kg insulin (Novolin ge Toronto; Novo Nordisk Canada, Mississauga, Ontario, Canada) was injected intraperitoneally with glucose measured at 0, 10, 20, 30, 60, 90, and 120 min.

Tissue Harvest and Immunohistochemistry
For tissue harvests, mice were fasted for 4 h and blood collected by cardiac puncture under isoflurane anesthesia, followed by cervical dislocation. Insulin (ALPCO Mouse Ultrasensitive Insulin ELISA; ALPCO, Salem, NH) and leptin (Mouse Leptin ELISA Kit; Crystal Chem, Downers Grove, IL) were measured in plasma. Tissues were immediately dissected, weighed, stored in 4% paraformaldehyde (pH 7.4) overnight, and then transferred to 70% ethanol. Tissues were paraffin-embedded and sectioned at 5 μm by Wax-it Histology Services Inc. (Vancouver, British Columbia, Canada), with hematoxylin-eosin (H-E) and Masson's trichrome staining on a subset of slides. Immunohistochemistry was performed as previously described (16) using rabbit insulin (1:200; #3014; Cell Signaling Technology, Danvers, MA) (RRID:AB_2126503) and mouse glucagon (1:1,000; #G2654; Sigma-Aldrich, St. Louis, MO) (RRID:AB_259852) antibodies. For β-cell mass analysis, three sections per sample, 200 μm apart, were stained and scanned on an ImageXpress Micro imager and analyzed with MetaXpress software (Molecular Devices, San

Jose, CA) by measuring thresholded insulin-positive area over pancreas area multiplied by pancreas mass. Islet mass was measured by multiplying pancreas mass by islet over pancreas area, determined from one scanned slide per mouse, and analyzed using ImageJ 1.52v.

Statistical Analyses
Measures at P35 were collected in parallel from males and females, and data were analyzed as two-way ANOVAs for factors of sex and treatment. For single time point measures in older mice, experiments in males and females were conducted separately at different ages and/or from different cohorts; thus, one-way ANOVAs were conducted within each sex. Mixed-effects models within each sex were used for all time course data. Tukey correction for multiple comparisons was used for all post hoc comparisons. For Figs. 2 and 3 and Supplementary Fig. 2, in which only four of eight groups are shown for clarity, statistical analyses were performed on all eight groups with Tukey correction for multiple comparisons. Correlations were assessed by Pearson correlation coefficients. Statistical analyses were performed using GraphPad Prism 8, with significance defined as $P < 0.05$.

Data and Resource Availability
All data generated or analyzed during this study are included in the published article (and its Supplementary Material online). No applicable resources were generated or analyzed during the current study.

RESULTS
Preweaning and Peripubertal HFD in Adolescent Males and Females
In mice examined until adolescence at P35 (Fig. 1A) (i.e., no P35 diet switch), both male and female HFD[P2–21] and HFD[P2+] offspring had higher body weights than CHOW and HFD[P21+] counterparts (Fig. 1B and C) from P5 to P25. Insulin tolerance tests at P30 (Fig. 1D and E) revealed that HFD[P2+] males had a faster return toward basal glucose compared with CHOW after insulin administration, but females overall had a higher area under the curve (AUC) compared with males (Fig. 1F), indicative of lower insulin sensitivity at this age. By P35 (Table 1), male body weights were overall higher than females (main effect of sex, $P < 0.0001$) but were no longer significantly different among groups. While there was no sex difference in fat pad weights, HFD[P2+] females had higher adiposity than CHOW females, reflected in gonadal (gWAT) (Fig. 1G), mesenteric (mWAT) (Table 1), and retroperitoneal white adipose tissue (rpWAT) (Table 1) weights. Peripubertal HFD in the HFD[P21+] group also increased gWAT and rpWAT weight in females (Fig. 1G and Table 1), but leptin levels were not significantly different among females (Fig. 1H) and were correlated with adipose tissue weights ($r = 0.7864$, $P < 0.0001$ for gWAT; $r = 08312$, $P < 0.0001$ for mWAT; and $r = 0.6229$, $P = 0.0011$ for rpWAT). Despite a lack of difference
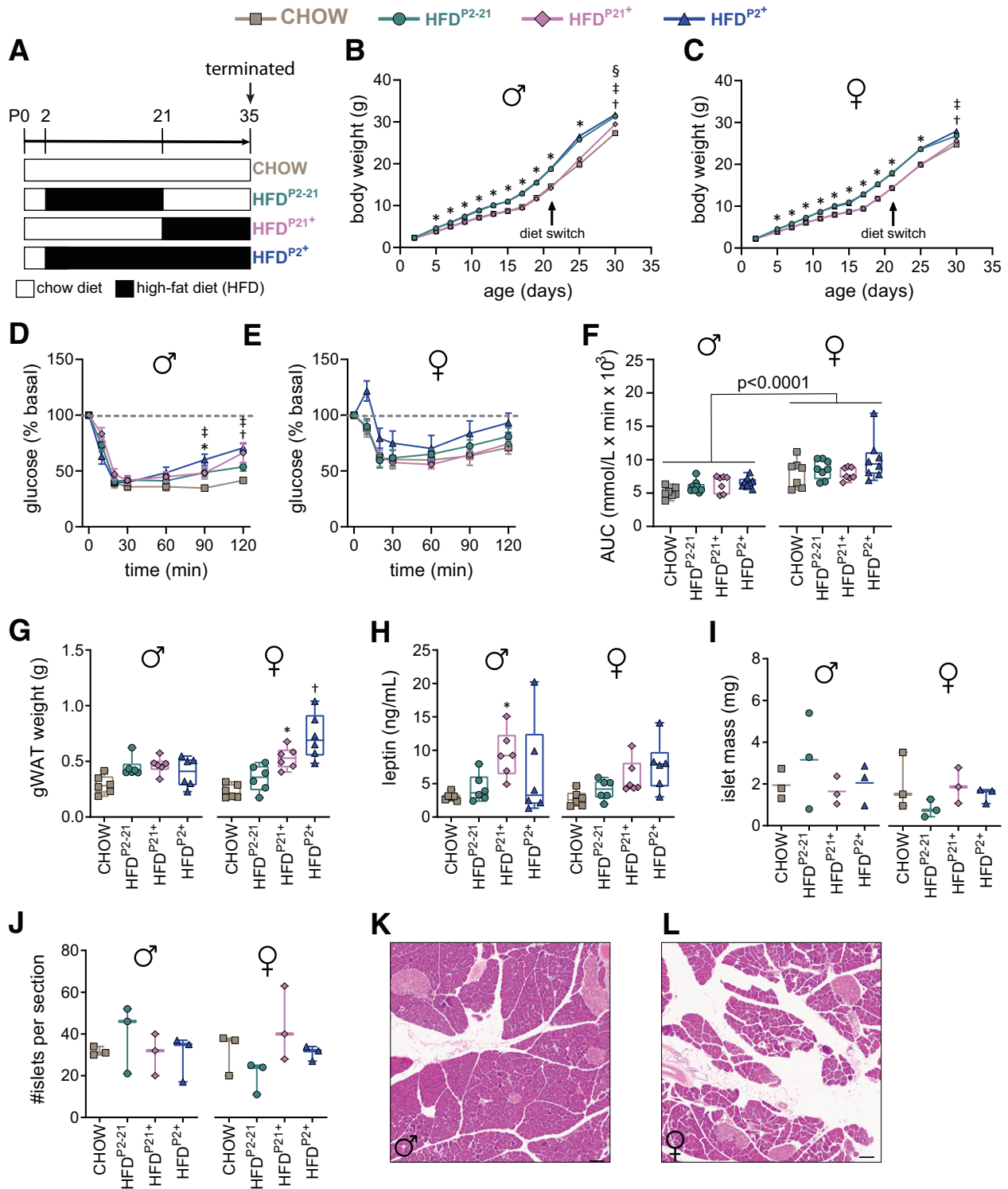
Figure 1—Preweaning and peripubertal HFD effects in adolescent males and females. *A*: Schematic of diet treatment groups for mice terminated at P35. Dams were maintained on chow diet (14 kcal% fat, designated by white bars) through pregnancy and until P2, at which time some dams were placed on HFD (45 kcal% fat, designated by black bars). Pups were weaned at P21 and either kept on the same diet as their mothers (CHOW and HFD^{P2+} groups) or diet was switched (HFD$^{P2–21}$ and HFD^{P21+}groups). *B*: Growth curves of male offspring from P2 to 30: *HFD^{P2+} and HFD$^{P2–21}$ > HFD^{P21+} and CHOW, *P* values <0.001; †HFD^{P21+} > CHOW, *P* < 0.05; ‡HFD^{P2+} and HFD$^{P2–21}$ > CHOW, *P* values <0.001; §HFD^{P2+}and HFD$^{P2–21}$ > HFD^{P21+}, *P* values <0.05. *n* = 17–20/group. *C*: Growth curves of female offspring from P2 to 30: *HFD^{P2+} and HFD$^{P2–21}$ > HFD^{P21+} and CHOW, *P* values <0.005; †HFD^{P2+} > HFD^{P21+}, *P* < 0.005; ‡HFD^{P2+} and HFD$^{P2–21}$ > CHOW, *P* values <0.005. *n* = 18–20/group. Glucose responses (normalized to 0 min value) during insulin tolerance tests in male (*D*) and female (*E*) offspring at P30–31 (*HFD$^{P2–21}$ > CHOW, *P* < 0.05; †HFD^{P2+} > HFD$^{P2–21}$, *P* < 0.05; ‡HFD^{P2+} > CHOW, *P* < 0.01) and corresponding AUC measures (*F*). *G*: gWAT weight in P35 males and females, left fat pad only. *HFD^{P21+} > CHOW and HFD$^{P2–21}$, *P* values <0.05; †HFD^{P2+} > CHOW, HFD^{P21+}, and HFD$^{P2–21}$, *P* values <0.05. *H*: Plasma leptin levels in P35 males and females. *HFD^{P21+} >

in adipose tissue weight among male groups, HFD^{P21+} males had higher leptin levels than chow males. Interestingly, HFD^{P2+} males had lower leptin levels despite longer exposure to HFD. Leptin levels are typically proportional to fat mass, and indeed, we did see a positive correlation between leptin and mass of gWAT ($r = 0.6353$; $P = 0.0009$), mWAT ($r = 0.7022$; $P = 0.0001$), and rpWAT ($r = 0.6204$; $P = 0.0012$). Liver weight was overall higher in males versus females and, when normalized to body weight, was highest in CHOW males and females (Table 1). Islet mass and islet number per section did not differ among groups nor between males and females, and islet morphology was similar in all mice (Fig. 1I–L). In addition, no sex or group differences were observed in fasting insulin levels (Table 1).

Timing of Dietary Fat During Development Impacts Body Weight and Diabetes Incidence

Body weights at P66 (Supplementary Fig. 1B and C) were significantly higher in males versus females (main effect of sex, $P < 0.0001$), with higher levels in HFD^{P21+} and HFD$^{P2–35}$ males compared with CHOW and higher body weight in HFD$^{P2–21,P35+}$ females compared with CHOW and HFD$^{P21–35}$. In males, all groups had at least one diabetic mouse with highest incidence in HFD$^{P2–21,P35+}$ and HFD^{P2+} males (Supplementary Fig. 1D). In contrast, after tracking fasting glucose to P316, only one female, from the HFD^{P35+} group, developed diabetes (Supplementary Fig. 1E). Interestingly, three other females (one HFD^{P21+}, one HFD^{P35+}, and one HFD^{P2+}) had transient elevations in fasting glucose in the 16 to 19 mmol/L range but returned to normal levels. Otherwise, females maintained normal fasting glucose levels throughout life.

Effects of Preweaning and Peripubertal HFD on Glucose Homeostasis

Monitoring of diabetes incidence, glucose tolerance, and insulin tolerance was performed in males and females of all eight treatment groups, and statistical analyses were performed with all eight groups within each sex to correct for multiple comparisons. However, for clarity, we present the data as groups of four in order to address specific questions, with the same CHOW and HFD^{P2+} groups included in all as controls. Figure 2 addresses the role of HFD exposure that is limited to early development, either just the preweaning period (HFD$^{P2–21}$) or extending through the peripubertal period (HFD$^{P2–35}$) (Fig. 2A). Diabetes incidence (Fig. 2B) was highest in the HFD^{P2+} group and lowest in the CHOW and HFD$^{P2–35}$ groups, with intermediate incidence in the HFD$^{P2–21}$ group. Glucose (Fig. 2C and D) and insulin (Fig. 2E and F) tolerance were not impaired by HFD limited to preweaning (P2–21)

or extending through puberty (P2–35), with only HFD^{P2+} females showing glucose impairment. Notably, unlike at P30 when HFD^{P2+} females had poor insulin sensitivity compared with males, at P66, all females had a robust insulin response with AUCs overall lower in females versus males (main effect of sex, $P = 0.0033$). When mice on chow diet were transiently placed on HFD only during the 2-week peripubertal period (HFD$^{P21–35}$ group), diabetes incidence, glucose tolerance, and insulin sensitivity were similar to CHOW mice that had remained on normal chow throughout life (Supplementary Fig. 2). Similarly, mice on HFD that were placed on normal chow only during the peripubertal period (HFD$^{P2–21,P35+}$ group) had similar diabetes incidence, glucose tolerance, and insulin sensitivity to HFD^{P2+} mice that were on HFD throughout life. Thus, a brief peripubertal diet switch did not impact these measures.

Timing of HFD Onset Affects Glucose Homeostasis and Diabetes Incidence

Compared with continuous HFD exposure throughout life, postponing HFD onset reduced and delayed diabetes incidence (Fig. 3A and B) with a greater delay seen when HFD was initiated at P35 (HFD^{P35+} group) compared with P21 (HFD^{P21+}). Despite the improvements in diabetes susceptibility, however, HFD^{P35+} males (Fig. 3C) had a mild impairment in glucose tolerance, such that glucose levels remained higher at the 120-min time point relative to CHOW males. However, this group difference was not reflected in corresponding AUCs likely due to the difference occurring at only the one time point. In females, mild impairments in glucose tolerance were observed in the HFD^{P21+}, HFD^{P35+}, and HFD^{P2+} groups relative to CHOW (Fig. 3D); however, only HFD^{P2+} females had a corresponding significant increase in AUC. Similar to glucose tolerance, HFD^{P35+} males had elevated glucose levels at a single time point (60 min) during an insulin tolerance test (Fig. 3E), with a faster return toward baseline relative to CHOW suggesting reduced insulin sensitivity. However, this difference again was not reflected in AUC. Females all showed similar glucose responses during the insulin tolerance test (Fig. 3F).

Effects of Diet Exposure on Plasma Hormones and Metabolic Tissues in Adult Males

There were no differences in insulin levels among the eight treatment groups at P47 (Fig. 4A). Insulin increased overall at P80 relative to P47, with higher levels mainly seen in mice that were on HFD postpuberty, including increases in HFD^{P35+}, HFD$^{P2–21,P35+}$, and HFD^{P2+} compared with other groups. However, β-cell mass did not

CHOW, $P < 0.05$. Islet mass (I) and number of islets per section (J) in P35 males and females (lines represent mean). Representative H-E pancreas sections from HFD^{P2+} male (K) and HFD^{P2+} female (L) at P35. Scale bars = 100 μm. Body weights in B and C are in nonfasted mice except for P30, which followed a 4-h fast. Arrow in B and C indicates age (P21) of diet switch in HFD$^{P2–21}$ and HFD^{P21+} mice. Body weight and glucose responses are mean ± SEM. Boxes in AUC and tissue weight panels represent interquartile range with line at the median, and whiskers represent minimum and maximum values.

Table 1—P35 measures

Measure/tissue	Males				Females			
	CHOW	HFD^P2−21	HFD^P21+	HFD^P2+	HFD^P2−21	CHOW	HFD^P21+	HFD^P2+
Body weight (g)*	31.5 (27.2–33.2)	33.9 (32.5–36.0)	33.8 (32.4–35.5)	33.1 (30.5–36.3)	27.5 (26.4–28.9)	25.9 (23.5–27.6)	26.9 (26.0–27.9)	28.7 (27.1–31.1)
Blood glucose (mmol/L)	7.3 (5.9–8.1)	5.8 (5.3–6.5)	7.2 (6.4–8.0)	7.1 (5.5–9.7)	6.6 (6.1–7.0)	6.9 (6.0–7.3)	6.8 (6.6–7.5)	7.4 (6.6–8.1)
mWAT weight (g)	0.237 (0.213–0.293)	0.309 (0.288–0.369)	0.369 (0.290–0.413)	0.250 (0.229–0.580)	0.289 (0.283–0.344)	0.250 (0.129–0.331)	0.363 (0.282–0.412)	0.395† (0.304–0.503)
rpWAT weight (g)	0.089 (0.078–0.099)	0.096 (0.090–0.128)	0.119 (0.109–0.130)	0.092 (0.057–0.134)	0.083 (0.073–0.107)	0.069 (0.057–0.075)	0.105‡ (0.097–0.122)	0.117† (0.108–0.137)
Liver weight (g)*	1.889 (1.613–2.030)	1.856 (1.677–2.013)	1.771 (1.660–1.857)	1.682 (1.564–1.964)	1.352 (1.105–1.508)	1.415 (1.210–1.587)	1.090 (1.063–1.166)	1.212 (1.083–1.399)
Liver weight (mg/g bw)*	60.46§ (57.24–62.39)	54.20 (50.08–57.59)	52.16 (50.07–55.01)	51.78 (49.94–53.03)	49.85 (41.49–51.73)	52.92# (51.42–59.30)	41.31 (40.07–42.54)	41.97 (39.60–45.14)
Insulin (ng/mL)	0.294 (0.198–0.448)	0.269 (0.195–0.350)	0.969 (0.729–1.451)	0.371 (0.206–0.856)	0.460 (0.350–0.693)	0.411 (0.324–0.489)	0.451 (0.352–0.649)	0.566 (0.493–0.680)

Data are median (interquartile range). n = 6/group. bw, body weight. *Significant main effect of sex, male > female: $P < 0.0001$; †female HFD^P2+ > CHOW, $P < 0.05$; ‡female HFD^P21+ > CHOW, $P < 0.05$; §male CHOW > HFD^P21+ and HFD^P2−21 and HFD^P2+, P values <0.05; #female CHOW > HFD^P2−21, HFD^P21+, and HFD^P2+, P values <0.05.

differ among groups and islet architecture as well as insulin and glucagon immunoreactivity were similar among all groups (Fig. 4B–D). β-Cell mass was, however, positively correlated to gWAT weight ($r = 0.530$; $P = 0.002$) and body weight ($r = 0.364$; $P = 0.040$), suggesting some ability of β-cells in males to compensate for HFD-induced obesity. Since HFD typically increases adiposity and leptin levels, it is not surprising that mice consuming HFD postpuberty had elevated leptin levels relative to groups consuming normal chow postpuberty (Fig. 4E). Unexpectedly, HFD^P2+ males that consumed HFD throughout life did not show such an elevation. Plasma leptin levels are typically proportional to fat mass, but we did not observe differences in gWAT (Fig. 4F) or mWAT (Fig. 4G) weights among treatment groups and leptin levels remained elevated after normalizing to body weight, in HFD^P21+, HFD^P35+, and HFD^P2−21,P35+ mice relative to HFD^P2−21 and HFD^P21−35 ($P < 0.05$), with levels in HFD^P21+ also greater than in CHOW mice ($P < 0.05$). A similar pattern was observed with liver weight and liver steatosis (Fig. 4H–K) in which HFD^P35+, HFD^P21+, and HFD^P2−21,P35+ groups had higher liver weight and/or steatosis relative to mice on normal chow postpuberty and HFD^P2+ mice. Leptin levels were also positively correlated to percentage of liver steatosis ($r = 0.617$; $P = 0.0002$).

Glucose Homeostasis Remains Stable as Females Age

Despite continued weight gain as female mice aged, plasma insulin levels (Fig. 5A) did not change significantly and did not differ among treatment groups at P149 or P325. Insulin and glucose tolerance also remained relatively stable. Insulin tolerance tests (Fig. 5B–E) generated similar AUC measurements at P129 and P275, although HFD^P21+ females had the lowest insulin sensitivity. CHOW females had the best insulin sensitivity with a robust response persisting at P275. Glucose tolerance (Fig. 5F and G) did not differ among groups at P290 with similar overall AUC levels to P88 (Figs. 2 and 3 and Supplementary Fig. 2), suggesting that glucose tolerance remained similar as females aged. Body weight (Fig. 5H) was not statistically different among groups at P316.

Liver Steatosis, Dysfunctional Adipose Tissue, and Islet Hyperplasia in Aged Females

At P325, higher liver weight and extensive liver steatosis were seen in females maintained on HFD postpuberty (i.e., post-P35) and highest in HFD^P2−21,P35+ females that were exposed to chow diet for 2 weeks during puberty (Fig. 6A–D). Immune cell clusters were observed adjacent to veins within the liver in some mice (Fig. 6D and Supplementary Table 1), including those with mild or absent steatosis and all HFD^P21−35 mice (i.e., HFD exposure limited to the peripubertal period). Leptin levels were highest in HFD^P2−21,P35+ females (Fig. 6E). In P325 females, mWAT weight did not vary among groups (Fig. 6F). However, gWAT weight (Fig. 6G) was surprisingly
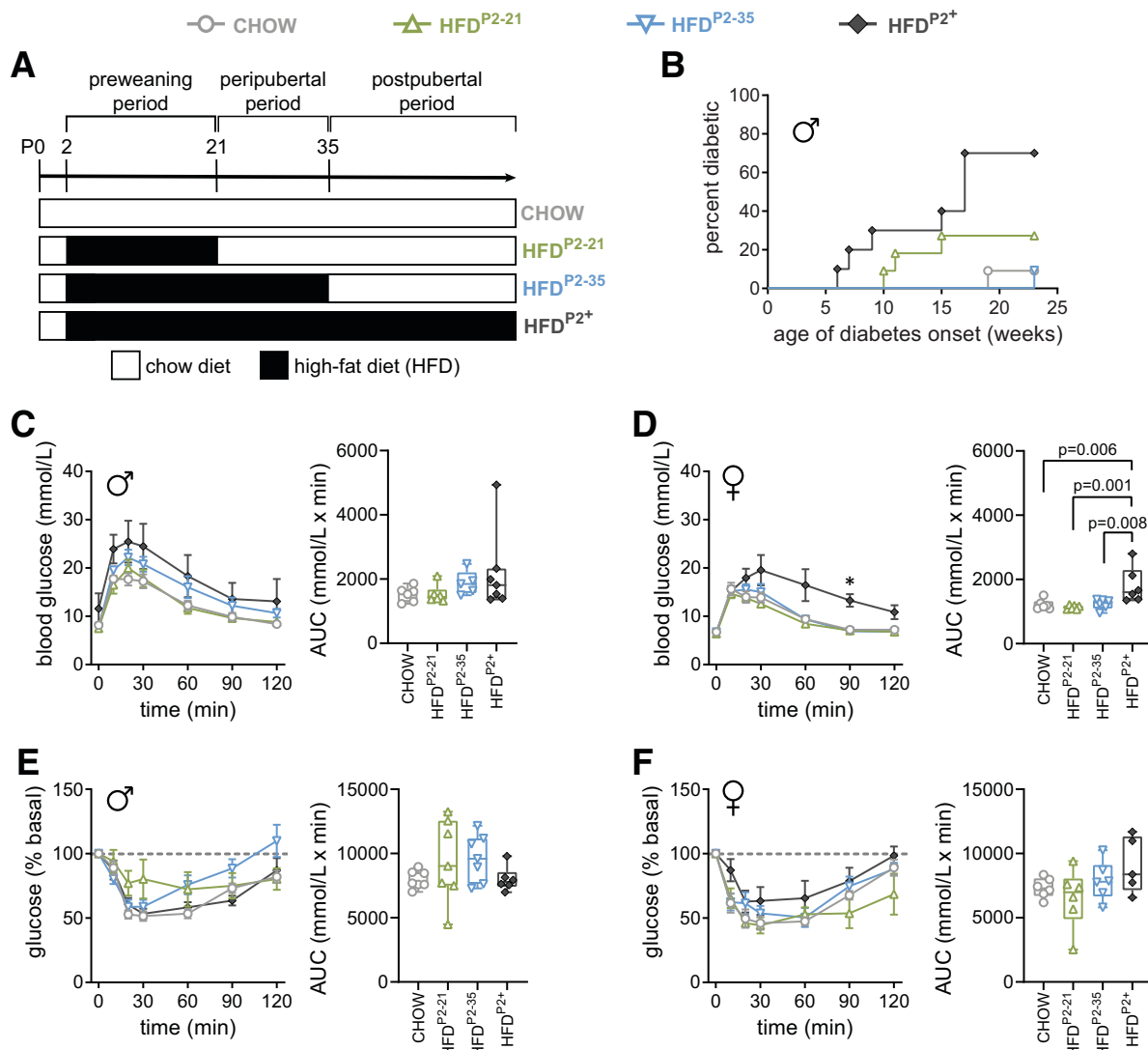
Figure 2—Effects of preweaning and peripubertal HFD on glucose homeostasis in adults. *A*: Schematic of diet treatment groups. Dams were maintained on chow diet (14 kcal% fat, designated by white bars) through pregnancy and until pup P2, at which time some dams were placed on HFD (45 kcal% fat, designated by black bars). Pups were weaned at P21. CHOW and HFD[P2+] pups were kept on the same diet as their mothers from P2 onwards. HFD[P2–21] offspring were switched from HFD to chow diet at P21, and HFD[P2–35] offspring were switched at P35. *B*: Diabetes incidence to 23 weeks of age in males. *n* = 10–11/group. HFD[P2+] > HFD[P2–35], *P* = 0.003; HFD[P2+] > CHOW, *P* = 0.003 by log-rank tests. Glucose response and AUC during oral glucose tolerance test in males at P50 (*C*) and females at P88 (*D*). *HFD[P2+] > HFD[P2–35], HFD[P2–21], and CHOW, *P* values <0.05. Glucose response and AUC during insulin tolerance test in males (*E*) and females (*F*) at P66. Note that data from CHOW and HFD[P2+] control groups are the same in Fig. 3 and Supplementary Fig. 2, with all statistical analyses controlling for multiple comparisons of all eight diet groups.

lower in HFD[P21+], HFD[P2–21,P35+], and HFD[P2+] females compared with CHOW females and generally lower in females consuming HFD postpuberty (i.e., post-P35). This lower gWAT weight was associated with gross abnormalities of fat pads (Supplementary Table 1) with a yellowish appearance as opposed to the typical white appearance. This was mainly observed in gWAT, but some mice also exhibited similar abnormalities in mWAT and perirenal WAT. Histological examination of abnormal gWAT by Masson's trichrome staining (Fig. 6*H*) revealed extensive fibrosis together with some enlarged adipocytes. H-E

examination of P325 female pancreas revealed a surprisingly high area covered by islets relative to acinar tissue in some mice (Fig. 6*I*). Islet architecture appeared normal with similarly robust insulin and glucagon staining among groups in P325 females (Fig. 6*J* and *K*). Analysis of islet mass revealed no significant differences among groups (Fig. 6*L*); however, some mice had remarkably high islet mass (up to 76 mg in an HFD[P2–21] mouse), although this was not consistent within treatment group. There was, however, a strong positive correlation between islet mass and AUC during insulin tolerance tests, both at P129 (*r* = 0.578;
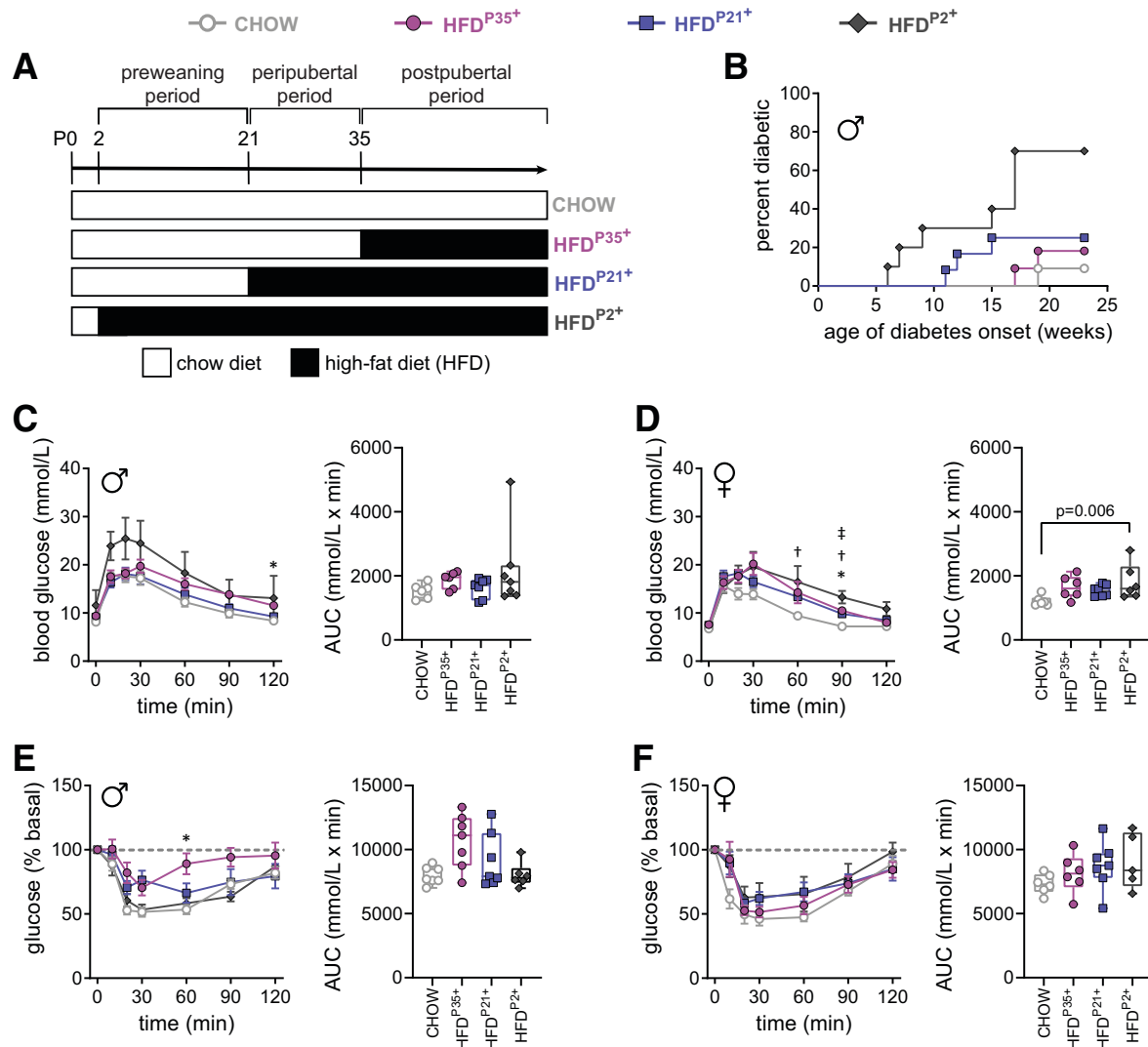
Figure 3—Timing of HFD onset affects glucose homeostasis and diabetes incidence in adults. *A*: Schematic of diet treatment groups. Dams were maintained on chow diet (14 kcal% fat, designated by white bars) through pregnancy and until pup P2, at which time some dams were placed on HFD (45 kcal% fat, designated by black bars). Pups were weaned at P21. CHOW and HFD^{P2+} pups were kept on the same diet as their mothers from P2 onwards. HFD^{P35+} offspring were switched to HFD at P35, and HFD^{P21+} offspring were switched to HFD at P21. *B*: Diabetes incidence to 23 weeks of age in males. n = 10–11/group. HFD^{P2+} > HFD^{P35+}, P = 0.009; HFD^{P2+} > HFD^{P21+}, P = 0.052; HFD^{P2+} > CHOW, P = 0.003 by log-rank tests. Glucose response and AUC during oral glucose tolerance tests in males at P50 (*C*) and females at P88 (*D*) and glucose response and AUC during insulin tolerance test in males (*E*) and females (*F*) at P66. *HFD^{P35+} > CHOW, P values <0.05; †HFD^{P21+} > CHOW, P values <0.05; ‡HFD^{P2+} > CHOW, P < 0.05. Note that data from CHOW and HFD^{P2+} control groups are the same in Fig. 2 and Supplementary Fig. 2, with all statistical analyses controlling for multiple comparisons of all eight diet groups.

P < 0.0001) and P275 (r = 0.585; P < 0.0001). Peri-insulitis was observed in some islets and was observed in all but the HFD^{P35+} group (Fig. 6*M* and Supplementary Fig. 3*A*), although only three mice remained in this group. Degree of insulitis was assigned a grade of 0 to 4, with no difference among treatment groups by grade (Supplementary Fig. 3*B*). However, grouping together all islets with any degree of insulitis together revealed highest levels in the HFD$^{P21–35}$ group (Fig. 6*N*), which were exposed to HFD only during 2 weeks peripuberty. Percent insulitis

was positively correlated to spleen weight even when normalized to body weight (r = 0.471; P = 0.002), and parallels were seen between treatment groups exhibiting immune cell accumulation in the liver and pancreas (Supplementary Table 1), suggesting a systemic inflammation. Although insulitis did not manifest as diabetes in females, we questioned whether Swiss Webster males may be prone to autoimmune destruction of β-cells despite not previously observing immune infiltration in male Swiss Webster islets. However, we did not observe cell proliferation of male Swiss
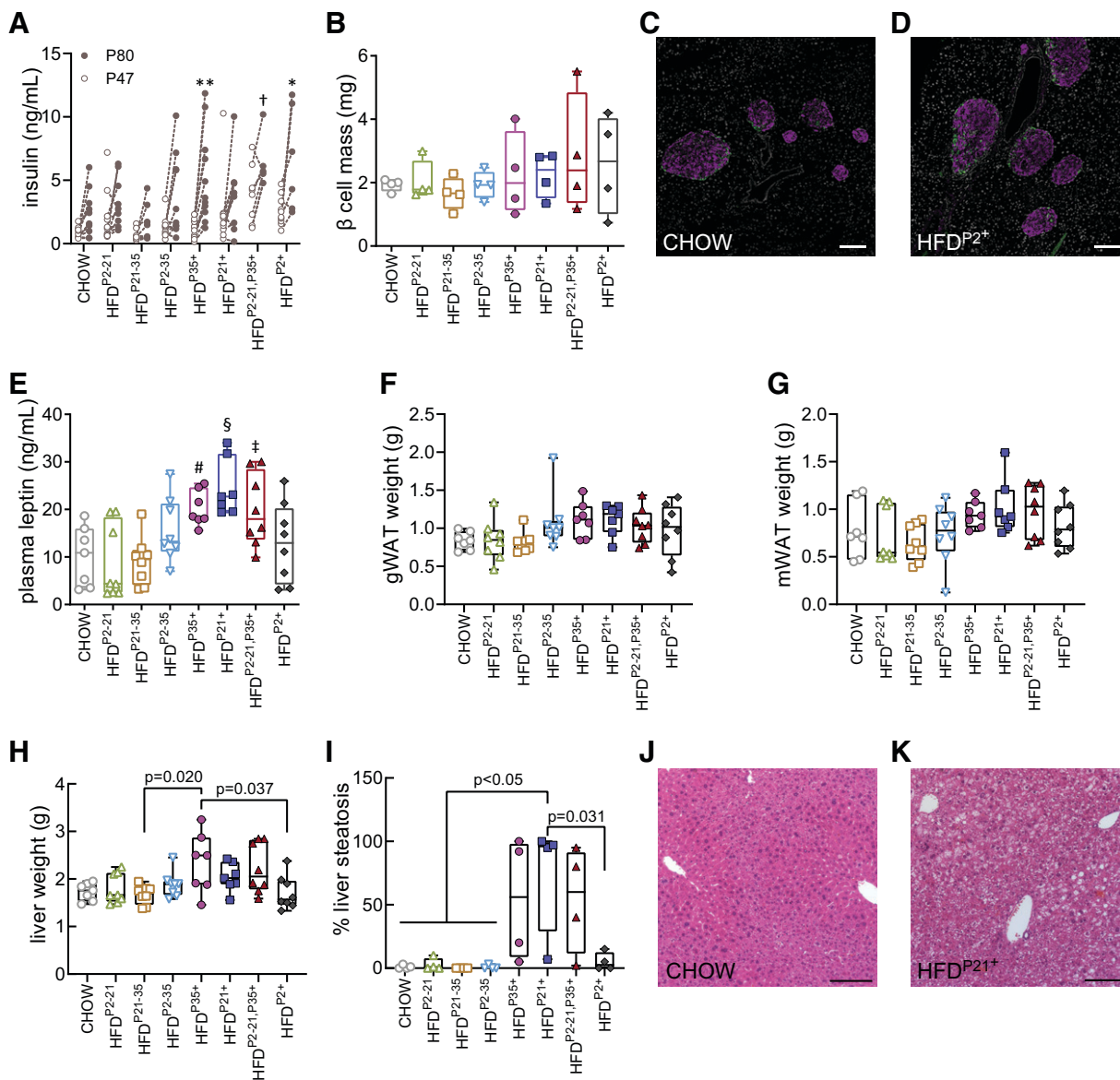
Figure 4—Effects of diet exposure on plasma hormones and metabolic tissues in adult males. *A*: Plasma insulin levels in males at P47 and P80. At P80, **HFD^{P35+} > HFD^{P21-35}, $P < 0.005$; †HFD$^{P2-21,P35+}$ > HFD^{P21-35} and CHOW, P values <0.05; *HFD^{P2+} > CHOW, HFD^{P2-21}, HFD^{P21-35}, and HFD^{P2-35}, P values <0.05, with no differences among treatment groups at P47 by mixed-effects analysis. Dotted lines connect values from the same mouse across age. *B*: β-Cell mass in males at P72 and representative pancreas sections of P72 males from CHOW group (*C*) and HFD^{P2+} group (*D*) with insulin in magenta, glucagon in green, and DAPI in white. *E*: Plasma leptin in P72 males: #HFD^{P35+}>HFD^{P21-35} and HFD^{P2-21}, P values <0.05; §HFD^{P21+} > CHOW, HFD^{P21-35}, HFD^{P2-21}, and HFD^{P2+}, P values <0.05; ‡HFD$^{P2-21,P35+}$ > HFD^{P21-35} and HFD^{P2-21}, P values <0.05. gWAT weight (*F*), mWAT weight (*G*), and liver weight (*H*) in P72 males. *I*: Percentage of liver section area, based on examination of H-E–stained slide, showing steatosis. Representative liver H-E sections of P72 males from CHOW group showing normal histology (*J*) and HFD^{P21+} group showing widespread steatosis (*K*). Scale bars = 100 μm. Insulin values are from cohort 1; remaining data are from cohort 2.

Webster splenocytes in response to insulin. Furthermore, administration of cyclophosphamide, at a dose that induces diabetes in NOD mice (29), did not induce diabetes in Swiss Webster males (Supplementary Fig. 4).

DISCUSSION

Detailed examination of the metabolic consequences of HFD exposure during various developmental time periods demonstrated the relative importance of dietary fat content during the preweaning, peripubertal, and postpubertal periods as well as marked sex differences. As we previously found, HFD consumption throughout life induced a high diabetes incidence in male Swiss Webster mice. We further found that incidence was earlier in mice when HFD was initiated at weaning (HFD^{P21+}) rather than postpuberty (HFD^{P35+}). This is unsurprising given
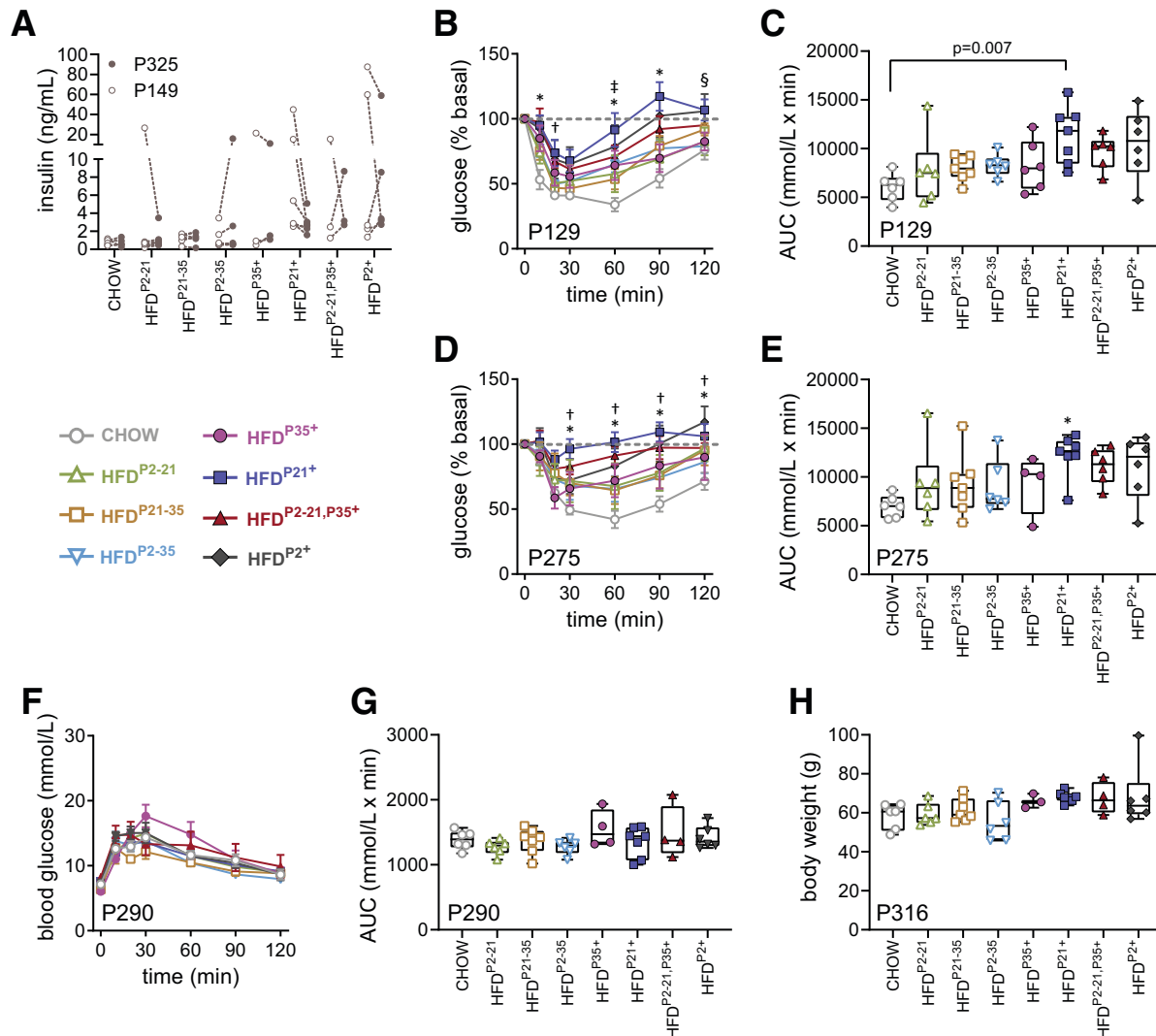
Figure 5—Glucose homeostasis remains stable as females age. *A*: Plasma insulin levels in females at P149 and P325. Insulin tolerance test and AUC in females at P129 (*B* and *C*) and P275 (*D* and *E*). *F* and *G*: Oral glucose tolerance test and AUC in females at P290. *H*: Body weight in females at P316; note that only three HFD^P35+ females and four HFD^P2–21,P35+ females remained at this age. *HFD^P21+ > CHOW, $P < 0.05$; †HFD^P2–21,P35+ > CHOW, $P < 0.05$; ‡HFD^P2–35 > CHOW, $P < 0.05$; §HFD^P2–21,P35+ > HFD^P2–35, $P < 0.05$.

the former was exposed to HFD for a longer time period. Notably, HFD exposure during just the preweaning period (HFD^P2–21) resulted in earlier onset and higher incidence of diabetes than if the HFD diet was extended through puberty (HFD^P2–35). This is unexpected given the shorter duration of HFD exposure in the former and that weaning to high-carbohydrate chow has previously been shown to promote β-cell proliferation and glucose responsivity of β-cells compared with weaning onto HFD (30). However, Vogt et al. (11) observed that HFD exposure during just the preweaning period resulted in impaired glucose tolerance and reduced parasympathetic outputs to islets with no difference in β-cell mass. Although we did not observe impaired glucose tolerance in HFD^P2–21 mice, we speculate that β-cells during the preweaning period are particularly sensitive to the detrimental effects of HFD,

rendering them susceptible to the added metabolic stressor of a sudden shift to a high-carbohydrate diet. Thus, while a nutrient switch at weaning may be an important trigger for β-cell maturation, it is also a vulnerable phase in β-cell development particularly in the presence of a genetic susceptibility to diabetes as in Swiss Webster males (16).

Delaying the initiation of HFD to postpuberty has previously been shown to promote adiposity and worsen insulin sensitivity (21,22). Although we did not observe a difference in adiposity, we did observe poorer insulin sensitivity when HFD was initiated in male mice postpuberty (HFD^P35+) instead of at weaning (HFD^P21+), despite being on HFD for a shorter time. Similar observations were made by Cordoba-Chacon et al. (22) in comparing mice with HFD initiation at 4 weeks relative to 12 weeks
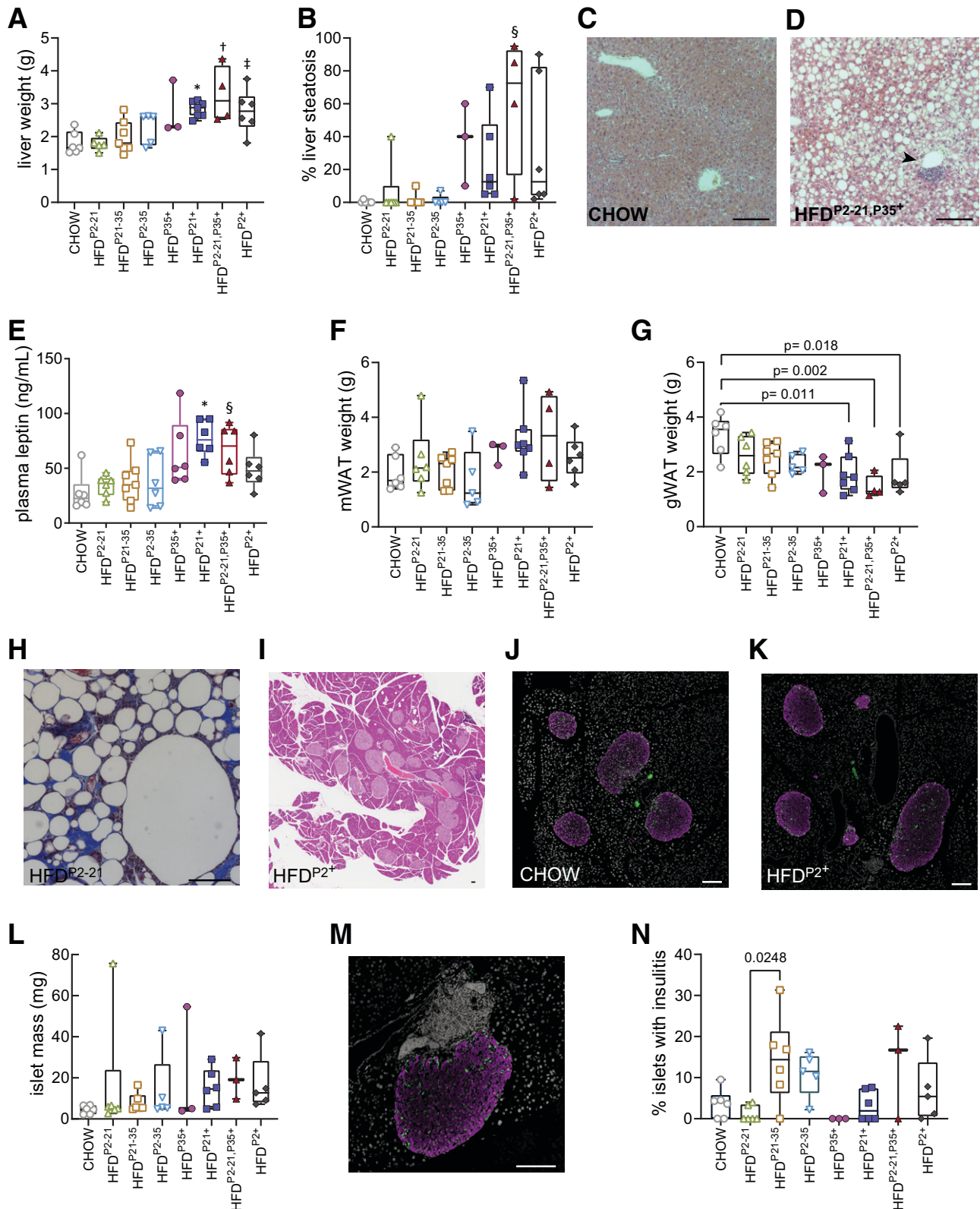
Figure 6—Liver steatosis, dysfunctional adipose tissue, and β-cell hyperplasia in aged females. Liver weight in P325 females (*A*) and percentage of liver section area (*B*), based on examination of H-E–stained slide, showing steatosis. *HFD^{P21+} > HFD^{P2-21} and CHOW, *P* values <0.05; †HFD$^{P2-21,P35+}$ > HFD^{P21-35}, HFD^{P2-21}, and CHOW, *P* values <0.01; ‡HFD^{P2+} > CHOW, *P* < 0.05; §HFD$^{P2-21,P35+}$ > HFD^{P2-35}, HFD^{P21-35}, HFD^{P2-21}, and CHOW, *P* values <0.05. Representative H-E–stained sections of CHOW liver (*C*) and HFD^{P2+} liver (*D*) in P325 females (arrowhead indicates vein with adjacent immune cell cluster). *E*: Plasma leptin levels in females at P149: *HFD^{P21+} > HFD^{P2-35}, HFD^{P2-21}, HFD^{P21-35}, and CHOW, *P* values <0.05; §HFD$^{P2-21,P35+}$ > CHOW, *P* < 0.05. mWAT weight (*F*) and gWAT weight (*G*) in P325 females. *H*: Masson's trichrome staining (blue = fibrosis) of fibrotic region of gWAT in an HFD^{P2-21} female at P325. *I*: Low-

of age. Interestingly, they found a greater lean mass when HFD was initiated earlier and speculated that this promoted insulin sensitivity and metabolic health. Although we did not measure lean mass in our mice, these findings suggest that HFD exposure during the critical peripubertal period of growth could actually have some beneficial effects on insulin sensitivity. In Swiss Webster male mice that are susceptible to HFD-induced diabetes, any beneficial effects on insulin sensitivity were insufficient to protect against primary β-cell failure, but an overall beneficial effect on metabolism may be more prominent in other strains.

Holtrup et al. (27) previously observed sustained glucose intolerance in response to brief HFD exposure during puberty in C57BL/6J males. In contrast, in our study, we did not see long-term metabolic impairments in either males or females in response to transient HFD exposure during puberty (HFD$^{P21–35}$). This discrepancy could be due to strain differences; however, since the study by Holtrup et al. (27) used a 60% fat diet, whereas our diet was 45% fat, a higher dietary fat content may be needed to see a long-term effect during puberty. Similarly, switching from HFD to chow diet only during puberty (HFD$^{P2–21,P35+}$ group) resulted in similar glucose and insulin tolerance compared with the HFD^{P2+} group in both sexes. We did not observe significant differences in β-cell mass among diet groups in males. However, there was greater variation in mice consuming HFD into adulthood, suggesting heterogeneity of metabolic responses in this outbred strain such that some mice but not others may be able to respond to metabolic stressors through expansion of β-cell mass. The mechanisms underlying such differential responses remain unclear.

We recently profiled plasma lipid species in Swiss Webster male mice via metabolomics and found alterations in response to HFD consumption, early overnutrition, and diabetes status (15) and highlighted the need for tissue-specific lipid analyses to understand the metabolic effects of these alterations. In the current study, we therefore examined liver steatosis as an index of long-term lipid dysregulation in this tissue. Postpubertal HFD exposure (i.e., after P35) promoted liver steatosis, with the surprising exception of male mice that were on HFD throughout life (HFD^{P2+} mice); thus, this was not only reflective of the longer length of HFD exposure. We and others have previously shown that leptin has an antisteatotic effect in the liver (31,32). However, this effect is lost in the state of leptin resistance (33), and, similar to what we observed in males in the current study, circulating leptin levels have been shown to correlate with severity of liver steatosis in humans (34). Although we would expect longer exposure to HFD to worsen lipid homeostasis, the lower

degree of liver steatosis in mice on HFD throughout life compared with shorter HFD exposure is in line with the Developmental Origins of Health and Disease hypothesis that metabolic systems adapt to the nutritional environment during development as a prediction of future dietary composition, but that an inaccurate prediction can result in maladaptation and adverse effects on metabolism (35). Thus, consistent exposure to HFD during development may have promoted adaptation to a high lipid environment with respect to liver steatosis. We therefore hypothesize that sudden changes in dietary macronutrient composition at critical points in development, specifically weaning and puberty, may lead to maladaptations in lipid regulation in comparison with a consistent diet, even when the diet is high in fat.

The striking sex differences observed in this study are particularly noteworthy. At P30, females showed reduced insulin sensitivity compared with males. However, insulin sensitivity improved in females after puberty and in fact showed greater sensitivity than males. This likely reflects the known transient insulin resistance that is seen during puberty (18,19). At P35, females also showed a greater HFD-induced increase in adiposity than males, specifically when HFD exposure included the peripubertal period (i.e., in HFD^{P21+} and HFD^{P2+} females) and higher than HFD exposure during the preweaning period (HFD$^{P2–21}$), despite the latter being a longer duration of exposure in pups terminated at P35. This suggests that females may be more sensitive than males to HFD-induced adipose growth during the peripubertal period and that HFD is more adipogenic in females during the peripubertal relative to the preweaning period. Although increased adiposity is generally thought of as unhealthy, appropriate adipose tissue expansion, particularly through adipocyte hyperplasia, can be an adaptive response that maintains metabolic health by allowing for appropriate storage of fats (36,37). We did not systematically assess adipocyte size and numbers, and it is not clear whether the higher adiposity in young females contributed a metabolic benefit. However, as discussed below, several females developed apparent adipose tissue dysfunction with age. Unlike the high diabetes incidence in males across several treatment groups, only one HFD^{P35+} female developed diabetes. Three other HFD-consuming females developed brief periods of hyperglycemia, but it was short-lived, indicating that their β-cells were able to adapt to the metabolic demand. This sex difference likely relates to the recognized protective role of estradiol in β-cell survival and function as well as protection from HFD-induced metabolic dysfunction (38,39). An ability of β-cells in Swiss Webster females to respond to metabolic demand was corroborated by examination of pancreas at 1 year of age that revealed an extremely high islet mass in several mice across

magnification image of pancreas section in an HFD^{P2+} female at P325 (insulin in magenta, DAPI in white) demonstrating β-cell hyperplasia. P325 female pancreas showing insulin (magenta), glucagon (green), and DAPI (white) in CHOW pancreas (*J*) and HFD^{P2+} pancreas (*K*). *L*: Islet mass in P325 females. HFD^{P2+} islet with peri-insulitis (*M*) and percent of islets per pancreas section (*N*) exhibiting peri-insulitis or insulitis. Scale bars = 100 μm.

treatment groups. The positive correlation between islet mass and AUC during insulin tolerance tests suggests that this islet expansion may be a response to insulin resistance. Although the temporal dynamics of this islet mass expansion are unknown, a previous study found massive islet hyperplasia in *ob/ob* mice at 1 year of age, with a near doubling from 26 to 52 weeks of age (40), suggesting that this could be a response to aging or prolonged obesity. Females also maintained normal glucose tolerance and insulin levels throughout life. HFD-consuming females exhibited a high degree of liver steatosis as well as fibrosis in WAT, particularly in the gonadal fat pad. Of possible relevance, a recent study by Kusminski et al. (41) using a transgenic model that induced adipocyte dysfunction and fibrosis in HFD-fed mice, triggered a similar degree of islet hyperplasia as we observed in some females, but in a short time frame, suggesting a potential proliferative signal from dysfunctional adipose tissue. If so, the adipose dysfunction we observed may have contributed to islet mass expansion that allowed HFD-consuming females to maintain normal glucose regulation. Insulitis was also observed in several females across all but the HFD^{P35+} treatment group. However, this did not appear to have any detrimental effects on glucose homeostasis, further supporting the compensatory capacity of β-cells in females.

Peri-insulitis is an early indicator of progression toward autoimmune diabetes in the NOD mouse (42). Although some Swiss Webster females exhibited peri-insulitis at 1 year of age, they remained normoglycemic. We have not previously observed peri-insulitis in any male Swiss Webster mice, but we wondered if an autoimmune component may contribute to their rapid onset of diabetes. However, we did not observe any sensitization of splenocytes to insulin in nondiabetic males. In addition, cyclophosphamide, at a dose that induces diabetes in NOD mice via depletion of Tregs (29,43), did not induce diabetes in Swiss Webster male mice. Thus, we found no indication of an autoimmune component to the diabetes phenotype of males. Several of the 1-year-old females also exhibited immune cell accumulation in liver, suggesting a more widespread inflammatory response rather than a specific autoimmune response against β-cells, perhaps related to aging.

In testing HFD exposure during various periods of postnatal development, rather than detrimental consequences that were consistent across all metabolic systems in response to specific timing patterns of HFD exposure, we observed that outcomes varied by metabolic parameter and tissue examined. Outcomes also differed considerably between males and females. Nonetheless, our studies suggest that both the preweaning and peripubertal periods are critical for metabolic programming and that dramatic changes in macronutrient composition of diet during these transitions can have significant impact on developmental trajectories of tissues. As such, careful consideration of the timing of dietary changes, sex differences, and the genetic background and susceptibility to metabolic impairments of the study model should be incorporated into experimental design of metabolic studies.

References

1. Teodoro JS, Varela AT, Rolo AP, Palmeira CM. High-fat and obesogenic diets: current and future strategies to fight obesity and diabetes. Genes Nutr 2014;9:406
2. Stein AD, Obrutu OE, Behere RV, Yajnik CS. Developmental undernutrition, offspring obesity and type 2 diabetes. Diabetologia 2019;62:1773–1778
3. Inadera H. Developmental origins of obesity and type 2 diabetes: molecular aspects and role of chemicals. Environ Health Prev Med 2013; 18:185–197
4. Friedman JE. Developmental programming of obesity and diabetes in mouse, monkey, and man in 2018: where are we headed? Diabetes 2018;67: 2137–2151
5. Perng W, Oken E, Dabelea D. Developmental overnutrition and obesity and type 2 diabetes in offspring. Diabetologia 2019;62:1779–1788
6. You S, Götz F, Rohde W, Dörner G. Early postnatal overfeeding and diabetes susceptibility. Exp Clin Endocrinol 1990;96:301–306
7. Plagemann A, Heidrich I, Götz F, Rohde W, Dörner G. Obesity and enhanced diabetes and cardiovascular risk in adult rats due to early postnatal overfeeding. Exp Clin Endocrinol 1992;99:154–158
8. Masuyama H, Hiramatsu Y. Additive effects of maternal high fat diet during lactation on mouse offspring. PLoS One 2014;9:e92805
9. Dearden L, Balthasar N. Sexual dimorphism in offspring glucose-sensitive hypothalamic gene expression and physiological responses to maternal high-fat diet feeding. Endocrinology 2014;155:2144–2154
10. Tsuduki T, Kitano Y, Honma T, Kijima R, Ikeda I. High dietary fat intake during lactation promotes development of diet-induced obesity in male offspring of mice. J Nutr Sci Vitaminol (Tokyo) 2013;59:384–392
11. Vogt MC, Paeger L, Hess S, et al. Neonatal insulin action impairs hypothalamic neurocircuit formation in response to maternal high-fat feeding. Cell 2014;156:495–509
12. Glavas MM, Kirigiti MA, Xiao XQ, et al. Early overnutrition results in early-onset arcuate leptin resistance and increased sensitivity to high-fat diet. Endocrinology 2010;151:1598–1610
13. Liang X, Yang Q, Zhang L, et al. Maternal high-fat diet during lactation impairs thermogenic function of brown adipose tissue in offspring mice. Sci Rep 2016;6:34345
14. Hafner H, Chang E, Carlson Z, et al. Lactational high-fat diet exposure programs metabolic inflammation and bone marrow adiposity in male offspring. Nutrients 2019;11:1393
15. Glavas MM, Hui Q, Miao I, et al. Early overnutrition in male mice negates metabolic benefits of a diet high in monounsaturated and omega-3 fats. Sci Rep 2021;11:14032
16. Glavas MM, Hui Q, Tudurí E, et al. Early overnutrition reduces Pdx1 expression and induces β cell failure in Swiss Webster mice. Sci Rep 2019;9:3619

17. World Health Organization. Healthy Diet Fact Sheet No. 394. 2015. Accessed 27 September 2021. Available from https://www.who.int/publications/m/item/healthy-diet-factsheet394

18. Moran A, Jacobs DR Jr, Steinberger J, et al. Insulin resistance during puberty: results from clamp studies in 357 children. Diabetes 1999;48:2039–2044

19. Kelsey MM, Zeitler PS. Insulin resistance of puberty. Curr Diab Rep 2016;16:64

20. Bjerregaard LG, Jensen BW, Ängquist L, Osler M, Sørensen TIA, Baker JL. Change in overweight from childhood to early adulthood and risk of type 2 diabetes. N Engl J Med 2018;378:1302–1312

21. Chu DT, Malinowska E, Jura M, Kozak LP. C57BL/6J mice as a polygenic developmental model of diet-induced obesity. Physiol Rep 2017;5:e13093

22. Cordoba-Chacon J, Gahete MD, Pozo-Salas AI, et al. Peripubertal-onset but not adult-onset obesity increases IGF-I and drives development of lean mass, which may lessen the metabolic impairment in adult obesity. Am J Physiol Endocrinol Metab 2012;303:E1151–E1157

23. Bohlen TM, Silveira MA, Zampieri TT, Frazão R, Donato J Jr. Fatness rather than leptin sensitivity determines the timing of puberty in female mice. Mol Cell Endocrinol 2016;423:11–21

24. Ullah R, Raza A, Rauf N, Shen Y, Zhou YD, Fu J. Postnatal feeding with a fat rich diet induces precocious puberty independent of body weight, body fat, and leptin levels in female mice. Front Endocrinol (Lausanne) 2019;10:758

25. Ramaley JA. Puberty onset in males and females fed a high fat diet. Proc Soc Exp Biol Med 1981;166:294–296

26. Pinter O, Beda Z, Csaba Z, Gerendai I. Differences in the onset of puberty in selected inbred mouse strains. Endocrine Abstracts 2007;14:P617

27. Holtrup B, Church CD, Berry R, et al. Puberty is an important developmental period for the establishment of adipose tissue mass and metabolic homeostasis. Adipocyte 2017;6:224–233

28. Klonoff DC, Parkes JL, Kovatchev BP, et al. Investigation of the accuracy of 18 marketed blood glucose monitors. Diabetes Care 2018;41:1681–1688

29. Yasunami R, Bach JF. Anti-suppressor effect of cyclophosphamide on the development of spontaneous diabetes in NOD mice. Eur J Immunol 1988;18:481–484

30. Stolovich-Rain M, Enk J, Vikesa J, et al. Weaning triggers a maturation step of pancreatic β cells. Dev Cell 2015;32:535–545

31. Lee Y, Wang MY, Kakuma T, et al. Liporegulation in diet-induced obesity. The antisteatotic role of hyperleptinemia. J Biol Chem 2001;276:5629–5635

32. Huynh FK, Neumann UH, Wang Y, Rodrigues B, Kieffer TJ, Covey SD. A role for hepatic leptin signaling in lipid metabolism via altered very low density lipoprotein composition and liver lipase activity in mice. Hepatology 2013;57:543–554

33. Fishman S, Muzumdar RH, Atzmon G, et al. Resistance to leptin action is the major determinant of hepatic triglyceride accumulation in vivo. FASEB J 2007;21:53–60

34. Polyzos SA, Aronis KN, Kountouras J, Raptis DD, Vasiloglou MF, Mantzoros CS. Circulating leptin in non-alcoholic fatty liver disease: a systematic review and meta-analysis. Diabetologia 2016;59:30–43

35. Gluckman PD, Hanson MA, Pinal C. The developmental origins of adult disease. Matern Child Nutr 2005;1:130–141

36. Vishvanath L, Gupta RK. Contribution of adipogenesis to healthy adipose tissue expansion in obesity. J Clin Invest 2019;129:4022–4031

37. Ghaben AL, Scherer PE. Adipogenesis and metabolic health. Nat Rev Mol Cell Biol 2019;20:242–258

38. Gannon M, Kulkarni RN, Tse HM, Mauvais-Jarvis F. Sex differences underlying pancreatic islet biology and its dysfunction. Mol Metab 2018;15:82–91

39. Morselli E, Criollo A, Rodriguez-Navas C, Clegg DJ. Chronic high fat diet consumption impairs metabolic health of male mice. Inflamm Cell Signal 2014;1:e561

40. Parween S, Kostromina E, Nord C, Eriksson M, Lindström P, Ahlgren U. Intra-islet lesions and lobular variations in β-cell mass expansion in ob/ob mice revealed by 3D imaging of intact pancreas. Sci Rep 2016;6:34885

41. Kusminski CM, Ghaben AL, Morley TS, et al. A novel model of diabetic complications: adipocyte mitochondrial dysfunction triggers massive β-cell hyperplasia. Diabetes 2020;69:313–330

42. Mohan JF, Kohler RH, Hill JA, Weissleder R, Mathis D, Benoist C. Imaging the emergence and natural progression of spontaneous autoimmune diabetes. Proc Natl Acad Sci USA 2017;114:E7776–E7785

43. Brode S, Raine T, Zaccone P, Cooke A. Cyclophosphamide-induced type-1 diabetes in the NOD mouse is associated with a reduction of CD4+CD25+Foxp3+ regulatory T cells. J Immunol 2006;177:6603–6612